Inactivation properties of T-type calcium current in canine cardiac Purkinje cells

Yuji Hirano, Harry A. Fozzard, and Craig T. January
Cardiac Electrophysiology Laboratories, Departments of Medicine (Cardiology) and Pharmacological and Physiological Sciences, The University of Chicago, Chicago, Illinois 60637

ABSTRACT The kinetic behavior of T-type Ca^{2+} current ($I_{Ca\text{-}T}$) was studied in canine cardiac Purkinje cells using a single suction-pipette whole-cell voltage clamp method. $I_{Ca\text{-}T}$ was studied without contamination of conventional L-type Ca^{2+} current ($I_{Ca\text{-}L}$). Ca^{2+}, Sr^{2+}, or Ba^{2+} were used as the charge carrier. During maintained depolarization $I_{Ca\text{-}T}$ decayed rapidly, and under most conditions the decay showed a voltage-dependent single exponential time course that did not depend on the species of charge carrier. The development of inactivation did not depend on Ca^{2+}, but the time course required more than a single exponential process. Just negative to the threshold voltage for activating $I_{Ca\text{-}T}$, inactivation slowly developed and there was a delay in its onset. The time course of recovery from inactivation was dependent on the protocol used to measure it. As the duration of an inactivating voltage step was increased, recovery slowed markedly and there was a delay in its onset. The time course of recovery could be fit as a biexponential. The fast and slow time constants of recovery were relatively constant, however, the relative amplitudes were dependent on the duration of the inactivating voltage step. Recovery was not dependent on Ca^{2+}, and it was slower at a less negative voltage. These results suggest that the T-type Ca^{2+} channel in cardiac Purkinje cells follows a complex kinetic scheme dependent only on voltage. This behavior can be accounted for by incorporating into a Markovian model several inactivated and closed states.

INTRODUCTION

Different properties of inactivation are one feature that distinguish some types of Ca^{2+} channels (see Fox et al., 1987*a* and *b*, for review). For L-type channels, the inactivation process is complex. For heart cells the time course of current decay after a depolarizing step depends on both the membrane voltage and Ca^{2+} (Kass and Sanguinetti, 1984; Lee et al., 1985). Recovery from inactivation of L-type Ca^{2+} current ($I_{Ca\text{-}L}$) exhibits a multiexponential time course and under certain conditions the peak current may exceed its steady-state value (see Tseng, 1988, for discussion). In contrast, the inactivation of T-type channels has appeared to be simpler. In most cell types the decay of T-type Ca^{2+} current ($I_{Ca\text{-}T}$) can be described by a single voltage-dependent time constant (Fedulova et al., 1985; Bossu et al., 1985; Carbone and Lux, 1987*a*; Fox et al., 1987*a*; Hagiwara et al., 1988; Hirano et al., 1989). Recovery from inactivation of $I_{Ca\text{-}T}$ has been reported to follow a single exponential process that depends on voltage (Carbone and Lux, 1987*a*; Hagiwara et al., 1988). However, in rat sensory neurones Bossu and Feltz (1986) found that two voltage-dependent time constants were required for recovery from inactivation of $I_{Ca\text{-}T}$, and they suggested a possible role for Ca^{2+} entry in modifying the slow component. A third Ca^{2+} current, the N-type, has been studied less extensively and it has not been reported in heart cells. In sensory neurones, its decay is reported to be voltage- and Ca^{2+}-dependent (Dupont et al., 1986; Fox et al., 1987*a*).

Recently, we described the presence of large amplitude currents through T- and L-type Ca^{2+} channels in cardiac Purkinje cells (Hirano et al., 1989). We showed that in this cell type $I_{Ca\text{-}T}$ and $I_{Ca\text{-}L}$ were separable by their voltage dependences of activation and inactivation, as well as by an array of drug and ionic interventions. The purpose of the present investigation was to study in detail the processes governing inactivation and recovery from inactivation of cardiac $I_{Ca\text{-}T}$. Our results show that the cardiac T-type Ca^{2+} channel is more complex and its kinetic description requires several inactivated and closed states.

A preliminary report of this work has appeared (Hirano et al., 1988).

METHODS

Preparation

Single canine cardiac Purkinje cells were isolated enzymatically as described previously (Sheets et al., 1983). Cells were maintained in Tyrode's solution and were used on the same day as isolated. Small aliquots of cells were transferred as needed to a chamber constructed on a glass coverslip and mounted on the stage of an inverted microscope (Diaphot, Nikon Inc., Garden City, NY). The temperature of the stage was thermostatically controlled at 30 ± 0.5°C.

Biophys. J. © Biophysical Society
Volume 56 November 1989 1007-1016
0006-3495/89/11/1007/10 $2.00

Electrical recordings and solutions

The voltage clamp technique was identical to that outlined previously (see Hirano et al., 1989, for details). Briefly, whole-cell membrane currents (Hamill et al., 1981) were recorded using a patch-clamp amplifier (model 8900, Dagan Corp., Minneapolis, MN). Current was sampled at 2–10 kHz by a 12-bit A/D converter (model DAC-02, Metrabyte Corp., Taunton, MA) under control of a laboratory computer (IBM-XT) and stored on a hard disk for subsequent analysis.

The experimental chamber was initially superperfused with a solution containing (in millimolar) NaCl 142, KCl 5.4, $CaCl_2$ 1.8, $MgCl_2$ 0.5, NaH_2PO_4 0.33, glucose 5.5, and Hepes 5 (pH adjusted to 7.4 with NaOH). Patch pipettes contained (in millimolar) CsCl 120, EGTA 10, MgATP 5, and Hepes 10 (pH adjusted to 7.3 with CsOH), and had resistances of 0.5–2.0 Mohm. In some experiments EGTA was replaced with Cs_4-BAPTA 5 and CsCl was lowered to 100 with no obvious change in the currents. Exchange between the pipette and cell interior was complete within 5–10 min of obtaining a seal to a cell and rupturing the patch, with the disappearance of transient and rectifying outward current. External solution was changed to Na^+-free solution containing (in millimolar) TEA-Cl 140, $MgCl_2$ 2, glucose 10, Hepes 10 (pH adjusted to 7.4 with TEA-OH), and tetrodotoxin (TTX, Sigma Chemical Co., St. Louis, MO) 0.01. The divalent cation used as charge carrier was added to this solution as indicated (2–20 mM of $CaCl_2$, $BaCl_2$ or $SrCl_2$) without osmotic correction. Under these conditions, Ca^{2+} channel currents could be studied without contamination by other membrane currents (see also Hirano et al., 1989).

Protocols and data analysis

Most experimental data are shown without subtraction of the capacity component (see Hirano et al., 1989, for method). Because $I_{Ca\text{-}T}$ decays rapidly and completely, the amplitude of $I_{Ca\text{-}T}$ was measured directly as the difference between the peak inward current and the steady current at the end of a 200-ms-long depolarizing step. Voltage clamp protocols (single depolarizing steps, double-pulse, and two-pulse protocols) were always applied at 0.1 Hz or less to permit full recovery.

Current decays were analyzed as a sum of exponentials by a Fourier method (Provencher, 1976) that determined the number of exponential components and their amplitudes and time constants. The time course of the onset of inactivation was studied using a double-pulse protocol and recovery from inactivation was studied using a two-pulse protocol. The exponentials describing these processes were determined using a nonlinear least-squares fitting routine to the peak currents (modified Gauss-Newton algorithm, Numerical Algorithm Group, Downers Grove, IL). Global convergence was tested using various starting values. Markovian model calculations were performed on an IBM-XT computer using Euler's method with an integration step size of 1 ms.

We used the terminology of Nowycky et al. (1985; see also Hirano et al., 1989) to describe the cardiac Ca^{2+} currents as long lasting (L-type, $I_{Ca\text{-}L}$) current and the transient (T-type, $I_{Ca\text{-}T}$) current.

RESULTS

Separation of T-type from L-type Ca^{2+} current

$I_{Ca\text{-}T}$ was separated from $I_{Ca\text{-}L}$ by its voltage dependence of activation and inactivation (see Hirano et al., 1989). As shown in the superimposed current traces in Fig. 1 *A*, a depolarizing test step (V_T) to −20 mV (lower traces) from a holding potential of −80 mV elicited a rapidly decaying inward current characteristic of $I_{Ca\text{-}T}$. In contrast, when $I_{Ca\text{-}T}$ was inactivated at a holding potential of −30 mV, the step to −20 mV elicited no inward current. Thus, for depolarizing steps up to −20 mV (20 mM $[Ca]_o$) or −30 mV (5 mM $[Ca]_o$) from more negative

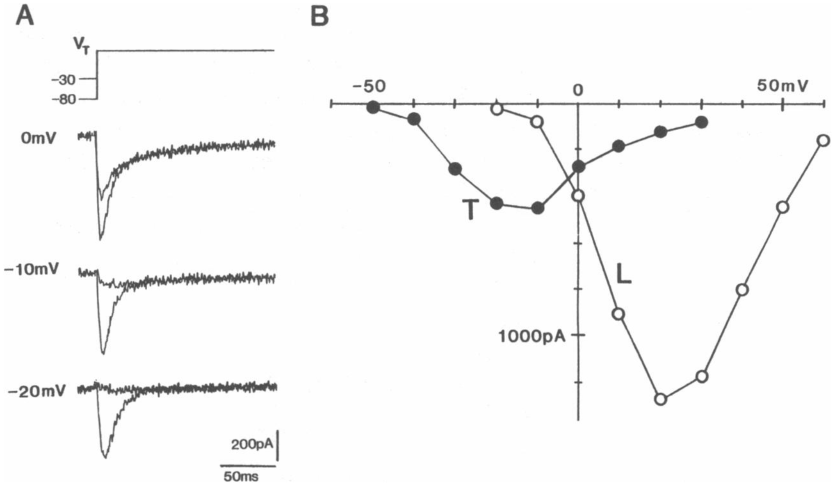

FIGURE 1 Separation of $I_{Ca\text{-}T}$ from $I_{Ca\text{-}L}$. (*A*) Ca^{2+} currents were elicited from holding potentials of −80 and −30 mV and superimposed. Voltages steps (V_T) to −20 mV (*bottom*) from a holding potential of −80 mV elicited $I_{Ca\text{-}T}$, whereas from holding potential of −30 mV no current was elicited. Steps to more positive V_T (−10 mV, *middle;* 0 mV, *top*) from a holding potential of −80 mV elicited both $I_{Ca\text{-}T}$ and $I_{Ca\text{-}L}$, and from a holding potential of −30 mV only $I_{Ca\text{-}L}$ was present. For these V_T, the difference current is $I_{Ca\text{-}T}$ which was observed only during the initial 50 ms. (*B*) Peak current-voltage relationships for $I_{Ca\text{-}T}$ and $I_{Ca\text{-}L}$. $[Ca]_o$ - 20 mM.

holding potentials $I_{\text{Ca-T}}$ could be shown directly. When stronger depolarizing test steps were applied to −10 mV (middle traces) or to 0 mV (upper traces) from a holding potential of −30 mV, a more slowly decaying current typical of $I_{\text{Ca-L}}$ was elicited. When depolarizing steps to these voltages were applied from a holding potential of −80 mV, additional inward current as $I_{\text{Ca-T}}$ was obtained, and it decayed within 50 ms to the $I_{\text{Ca-L}}$ baseline. Under these conditions, $I_{\text{Ca-T}}$ can be shown by subtracting the $I_{\text{Ca-L}}$ component (see also Hirano et al., 1989). Fig. 1 *B* shows the current-voltage plots of the peak $I_{\text{Ca-T}}$ and $I_{\text{Ca-L}}$ obtained in this cell (20 mM $[\text{Ca}]_o$).

In the studies reported here, the possibility of contamination by $I_{\text{Ca-L}}$ of the analysis of kinetics for $I_{\text{Ca-T}}$ was avoided by studying the voltage range negative to that where $I_{\text{Ca-L}}$ was activated.

Decay of $I_{\text{Ca-T}}$

During a maintained depolarization, $I_{\text{Ca-T}}$ decays rapidly usually with a single exponential time course. Fig. 2 shows semilogarithmic plots of $I_{\text{Ca-T}}$ decays for voltage steps to −40 and −30 mV. The records were obtained in the same cell, first in external solution containing 5 mM Ca^{2+} (upper panel), and then after switching to Ca^{2+}-free external solution containing 5 mM Sr^{2+} (lower panel). With both divalent charge carriers, the current amplitudes and their decays were similar. The currents decayed more rapidly at more positive voltages and the decays were a single exponential process. We obtained similar findings with replacement of Ca^{2+} by Ba^{2+}. Close to the threshold voltage for eliciting $I_{\text{Ca-T}}$ (−50 or −60 mV in 20 or 5 mM $[\text{Ca}]_o$, respectively), where the current amplitude was small, the results were less clear, and more than one exponential component was occasionally required to obtain the best fit.

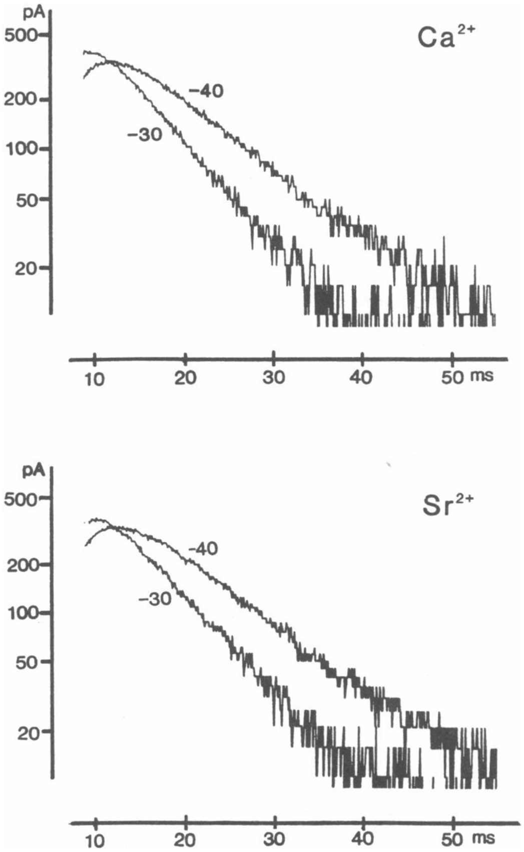

FIGURE 2 Semilogarithmic plot of the decay of $I_{\text{Ca-T}}$ with 5 mM Ca^{2+} (*top*) and Sr^{2+} (*bottom*) as the charge carrier. $I_{\text{Ca-T}}$ was obtained directly by depolarization to −30 and −40 mV from the holding potential of −80 mV. Decay time constants with Ca^{2+} were 10.9 ms at −40 mV and 7.0 ms at −30 mV, and with Ba^{2+} they were 11.9 ms at −40 mV and 7.7 ms at −30 mV.

Development of inactivation

The development of inactivation was examined near the threshold voltage for $I_{\text{Ca-T}}$ using the double-pulse protocol shown in Fig. 3 *A*. From a holding potential of −80 mV, the membrane was stepped to a conditioning voltage (V_c) for variable times (ΔT) before a depolarizing step was made to −30 mV to activate $I_{\text{Ca-T}}$. Current records for the same V_c, but with different ΔT were then superimposed. As shown in the current records in the top panel, the step to a V_c of −45 mV elicited $I_{\text{Ca-T}}$, which then rapidly decayed. After the step to −30 mV, additional $I_{\text{Ca-T}}$ was elicited; however, its peak amplitude rapidly declined at longer ΔT as T-type Ca^{2+} channels inactivated. For more negative V_c (−50 or −55 mV, second and third panels, respectively), the amplitude of $I_{\text{Ca-T}}$ was smaller and it decayed more slowly. After the subsequent step to −30 mV, the amplitude of $I_{\text{Ca-T}}$ gradually declined at longer ΔT as T-type Ca^{2+} channels inactivated. The extent of inactivation and its time course of development were steeply dependent on V_c. For a V_c to −60 mV (bottom panel), activation of $I_{\text{Ca-T}}$ was not observed. Nonetheless, a time-dependent decrease in the peak $I_{\text{Ca-T}}$ was present for the steps to −30 mV. This finding could suggest that the T-type Ca^{2+} channel is able to inactivate without first opening, and that this transition is kinetically slow. Fig. 3 *B* shows semilogarithmic plots of peak $I_{\text{Ca-T}}$ elicited with the voltage steps to −30 mV from the different V_c in the same cell. These results show that the time course of development of inactivation was not adequately fitted as a single exponential process, rather it was multiexponential. Exponential fit to the decline of peak current at each V_c usually could be described using two components. At a V_c of −45 mV, >90% of the current inactivated to a steady-state value, and it was complete within ~800 ms.

Hirano et al. Inactivation of $I_{\text{Ca-T}}$ 1009

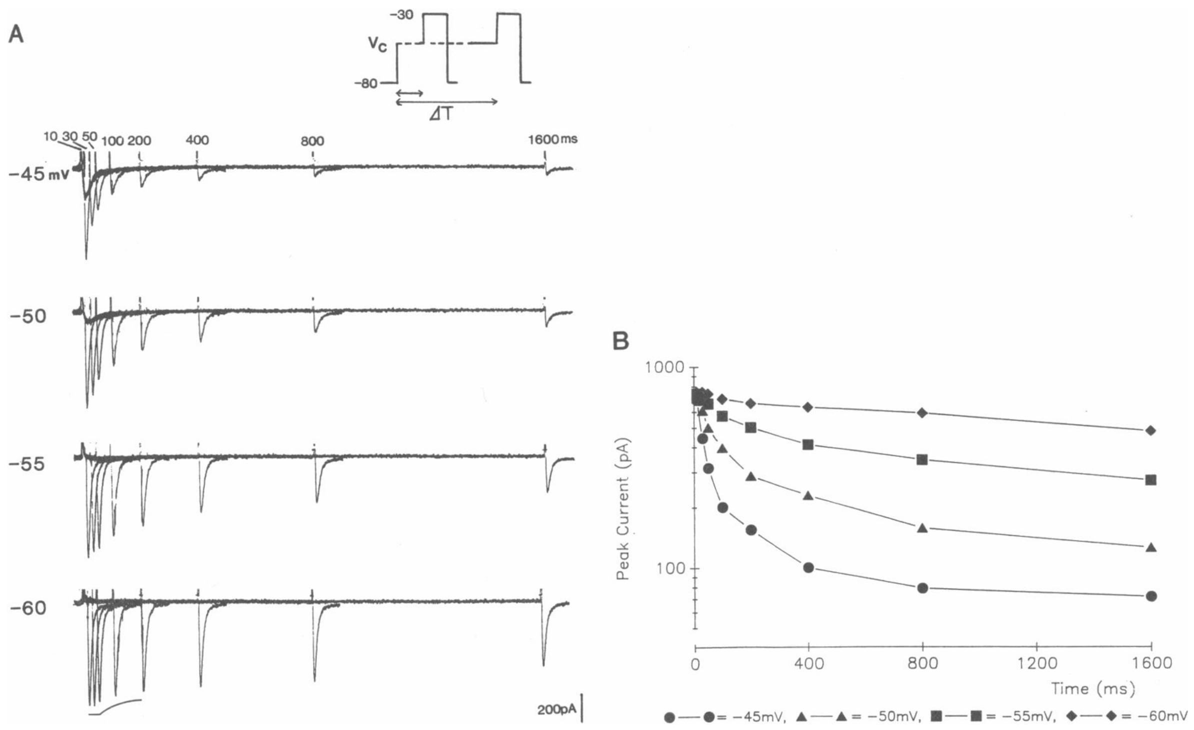

FIGURE 3 Development of inactivation of $I_{Ca\text{-}T}$ near threshold voltages. (*A*) Using a double-pulse protocol (*inset*), the availability of $I_{Ca\text{-}T}$ was determined by a voltage step to -30 mV after an initial step to a conditioning voltage (V_c) for variable time intervals (ΔT). Superimposed current traces for V_c to -45, -50, -55, and -60 mV are shown. At all V_c, the availability of $I_{Ca\text{-}T}$ decreased as T-type channels inactivated. See text for additional discussion. (*B*) Semilogarithmic plot shows development of inactivation of $I_{Ca\text{-}T}$. As V_c became more negative, inactivation slowed, and at all V_c it could not be fit as a single exponential process. $[Ca]_o = 20$ mM.

At more negative V_c, inactivation was less complete and its time course slowed dramatically.

An additional finding shown in Fig. 3 *A* is that at the V_c of -60 mV a delay was present before the onset of inactivation. The peak current amplitude elicited after the step to -60 mV for 10 and 30 ms were identical, and it was not until 50 ms of inactivation at -60 mV that the peak $I_{Ca\text{-}T}$ began to decline. This delay is emphasized by the solid line. The inclusion of a 5-ms-long repolarizing step to -80 mV before application of the step to -30 mV (see Gillespie and Meves, 1980) or the use of Ba^{2+} in place of Ca^{2+} did not alter these results ($n = 8$).

Recovery from inactivation

We used a two-pulse voltage clamp protocol to study recovery from inactivation of $I_{Ca\text{-}T}$. The protocol contained an initial step to -30 mV from the holding potential to activate and inactivate $I_{Ca\text{-}T}$. The membrane was then repolarized for a variable time interval (ΔT) before a second depolarizing step was applied to elicit $I_{Ca\text{-}T}$ that had recovered from inactivation. Fig. 4 shows superimposed current records of $I_{Ca\text{-}T}$ elicited with the second step of the two-pulse protocol. The time interval of recovery before application of the second step is indicated above each trace in the upper panel. In each panel the two-pulse voltage clamp protocol was identical except for the duration of the initial depolarizing step, and these protocols are shown to the left. When the initial depolarizing step duration was 50 ms (upper traces), $I_{Ca\text{-}T}$ recovered from inactivation rapidly. When the duration of this initial inactivating step was increased to 2,000 ms (middle traces), recovery slowed (note different current amplitude scales). When the holding potential was set to -30 mV (lower traces, "infinity" protocol with holding potential present >1 min), recovery from inactivation was further slowed.

In addition to slowing of the recovery time course with lengthening of the initial depolarizing step duration, the onset of recovery from inactivation also was delayed. With an initial depolarizing step duration of 50 ms a small amplitude $I_{Ca\text{-}T}$ was present with a recovery interval as short as 10 ms. In contrast, with the "infinity" protocol inward current was not obtained until 100 ms of recovery.

Recovery from inactivation also depended on the volt-

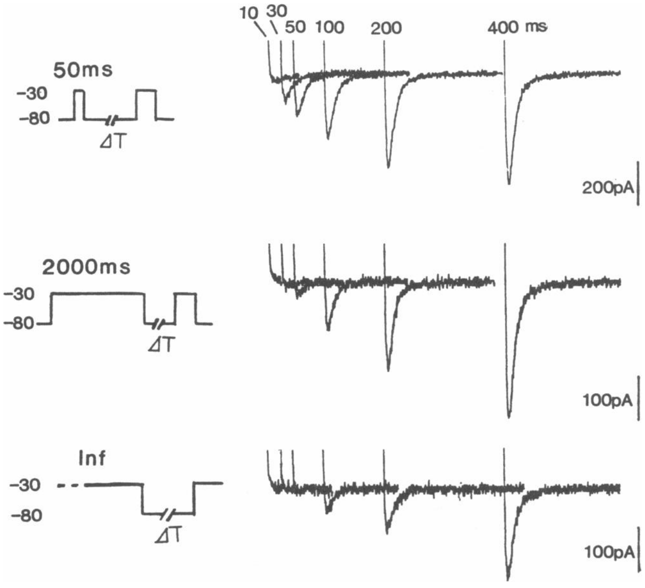

FIGURE 4 Dependence of the time course of recovery from inactivation of $I_{Ca\text{-}T}$ on the experimental protocol. Two-pulse protocols are shown (*left*) and resultant superimposed current traces (*right*). Lengthening the duration of the initial inactivating step from 50 ms (*top*) to 2,000 ms (*middle*) slowed the time course of recovery. Changing the holding potential to -30 mV ("infinity" protocol, *bottom*) further slowed the time course of recovery and there was a delay in its onset. $[Ca]_o = 20$ mM.

age of the recovery interval. The experimental protocols were similar to those used in Fig. 4. Plots of recovery from inactivation of peak $I_{Ca\text{-}T}$ at recovery interval voltages of -80 mV (*solid symbols*) and -60 mV (*open symbols*) are shown in Fig. 5 *A*. At the recovery interval voltage of -80 mV and with an initial depolarizing step duration of 50 ms, recovery from inactivation of $I_{Ca\text{-}T}$ was complete within 800 ms. When the initial depolarizing step duration was 2,000 ms, recovery from inactivation slowed but was nearly complete within 1,600 ms. With the "infinity" protocol recovery slowed further, and complete recovery required nearly 10 s (data not shown). When the recovery interval voltage was -60 mV, $I_{Ca\text{-}T}$ recovered from inactivation. However, the peak current amplitudes obtained with the two-pulse protocols were markedly reduced. The data for recovery at these voltages also were normalized (maximum peak current at 1,600 ms of recovery at -80 and -60 mV = 100%) and are replotted in Fig. 5 *B*. For each type of two-pulse protocol, recovery from inactivation was slower at a recovery voltage of -60 mV than at a recovery voltage of -80 mV ($n = 7$). These findings, along with those shown above, illustrate the critical dependence of the recovery process on the protocol used to study it.

Fig. 6 shows the time course of recovery from inactivation of $I_{Ca\text{-}T}$ and the effect of 20 mM Ca^{2+} (upper plot) or Ba^{2+} (lower plot) as the charge carrier. Using two-pulse protocols similar to those shown in Fig. 4 (recovery interval voltage, -80 mV), the peak current in response to the second depolarizing step was measured at different time intervals (ΔT) during recovery and plotted. The time course of recovery from inactivation slowed as the duration of the initial depolarizing step was lengthened, as was shown previously, and the results were similar for both Ca^{2+} or Ba^{2+}. With the "infinity" protocol, full recovery required nearly 10 s with both Ca^{2+} and Ba^{2+}.

We analyzed the time course of recovery using a nonlinear least-squares method. The peak $I_{Ca\text{-}T}$ amplitude (I_t) was obtained after variable recovery intervals and was normalized to the peak current obtained with the initial depolarizing step (I_c). For the "infinity" protocol, I_c was

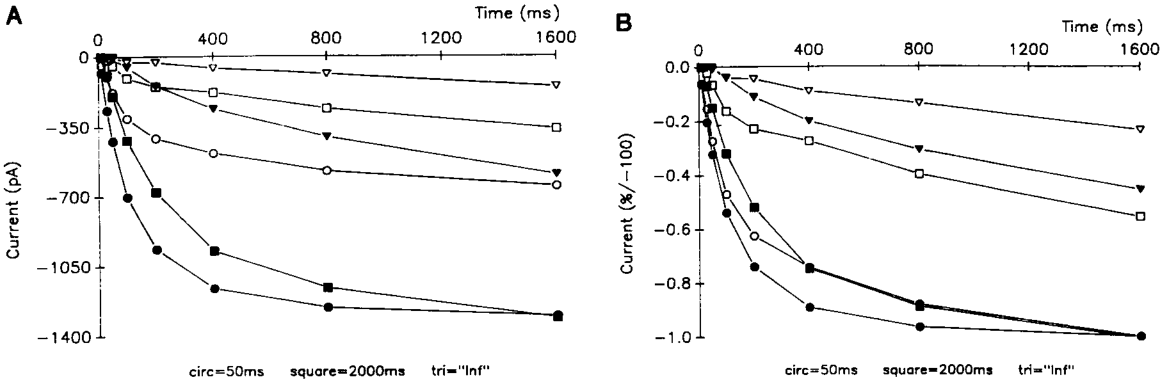

FIGURE 5 Dependence of recovery from inactivation of $I_{Ca\text{-}T}$ on recovery voltage. Two-pulse protocols were used to study recovery from inactivation at recovery voltages of -80 mV (*solid symbols*) and -60 mV (*open symbols*). Initial inactivating step durations of 50 and 2,000 ms and the "infinity" protocol were tested (see similar protocols in Fig. 4). (*A*) Plots of the peak currents show that $I_{Ca\text{-}T}$ recovered less at -60 mV than at -80 mV, and recovery of $I_{Ca\text{-}T}$ slowed as the duration of the inactivating step was lengthened at both recovery voltages. (*B*) Normalized peak currents are plotted and show that for each type of two-pulse protocol $I_{Ca\text{-}T}$ recovered more slowly at -60 mV than at -80 mV.

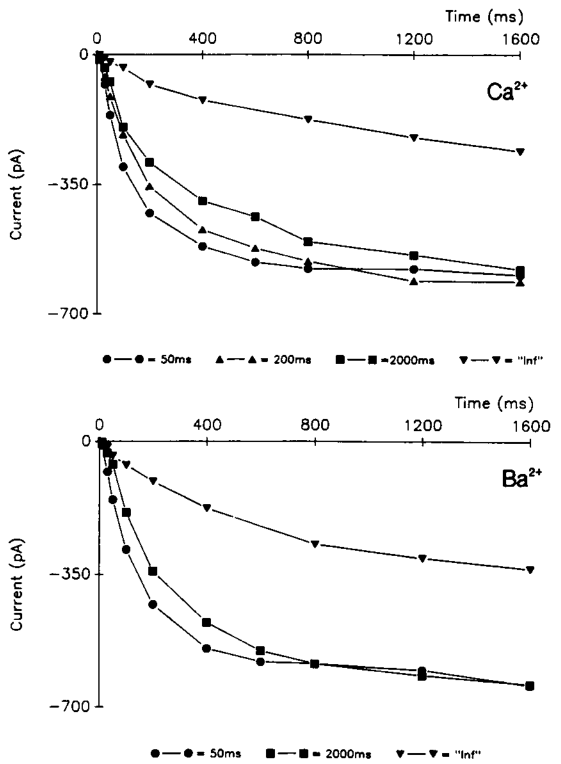

FIGURE 6 Time course of recovery with Ca^{2+} and Ba^{2+} as the charge carrier. Recovery from inactivation of T-type channel currents was determined using different two-pulse protocols (recovery voltage = −80 mV, initial inactivating step durations of 50, 200, 2,000 ms and "infinity" protocol). Plots of the time course of recovery in 20 mM $[Ca]_o$ (*top*) and 20 mM $[Ba]_o$ (*bottom*) show that the recovery process was independent of Ca^{2+}.

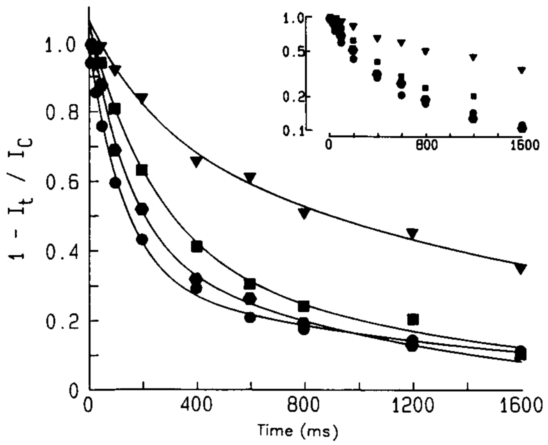

FIGURE 7 Double exponential fitting to the $I_{Ca\text{-}T}$ recovery time course. For each two-pulse recovery protocol, the recovery time course was normalized (see text). As the duration of the inactivating pulse was lengthened (●, 50 ms, ●, 200 ms; ■, 2,000 ms; ▼, "infinity" protocol), the time course of recovery slowed. Double exponential fit to the data is shown by the solid lines. For this cell t_{short} was 132, 141, 240, and 248 ms for inactivating step durations of 50, 200, 2,000 ms, and the "infinity" protocol. t_{long} was 688, 1,236, 1,481, and 1,887 ms, respectively. Semilogarithmic plot (*inset*) shows that recovery cannot be adequately fit as a single exponential process.

the peak current elicited after 20 s of recovery. The time course of recovery (plotted as $1 - I_t/I_c$) is shown in Fig. 7. Semilogarithmic plot of the data (see inset) shows that recovery cannot be adequately fit as a single exponential process. Rather, after the delay in the onset of recovery, the time course of recovery usually could be fitted as the sum of two exponentials (t_{long} and t_{short}). The double exponential fits to the data points are shown by the solid lines.

The results of double exponential fitting to the recovery time courses for six cells are summarized in Table 1. For each inactivating step duration studied, t_{long} and t_{short} and their relative amplitudes are given. The values for t_{long} and t_{short} were relatively similar among the cells. Furthermore, as the duration of the inactivating step was lengthened, the relative amplitude of the two time constants varied consistently. For inactivating step durations where the decay of $I_{Ca\text{-}T}$ was complete (i.e., ≥50 ms), the average value (mean ± SEM) for the relative amplitude of t_{long} increased from 0.263 ± 0.032, 0.430 ± 0.021, 0.457 ± 0.043, to 0.625 ± 0.035 for inactivating step durations of 50, 200, 2,000 ms, and the "infinity" protocol, respectively. For the same inactivating step durations, the average value for the relative amplitude of t_{short} decreased from 0.755 ± 0.040, 0.663 ± 0.043, 0.602 ± 0.051, to 0.315 ± 0.005. Thus, with lengthening of the duration of the inactivating voltage step, there was a consistent shift in recovery from a rapid process toward a slower one.

DISCUSSION

Separation of $I_{Ca\text{-}T}$ from $I_{Ca\text{-}L}$

The cardiac Purkinje cell possesses a prominent current carried by T-type Ca^{2+} channels, offering the opportunity to examine its kinetic properties in detail. In the present work, $I_{Ca\text{-}T}$ was separated from $I_{Ca\text{-}L}$ by its voltage dependence of inactivation and activation (Hirano et al., 1989). Because the amplitude of $I_{Ca\text{-}T}$ is large even at low Ca^{2+} concentrations, and $I_{Ca\text{-}T}$ was shown directly and not as a subtraction current, possible contamination from $I_{Ca\text{-}L}$ was avoided. Although this approach limited the voltage range over which $I_{Ca\text{-}T}$ could be studied, it is sufficient to determine several general characteristics of $I_{Ca\text{-}T}$ kinetics. A more precise distinction over a larger voltage range may be possible by studying single channel behavior (particularly with Ba^{2+} as charge carrier) where T- and

TABLE 1 $I_{Ca\text{-}T}$ **recovery time constants and relative amplitudes**

Experiment no.	Inactivating step duration	T_{long}	Amplitude	T_{short}	Amplitude
	ms	*ms*		*ms*	
1	50	730	0.19	111	0.87
	200	572	0.39	132	0.59
	2000	538	0.52	105	0.42
2	50	1651	0.31	116	0.73
	200	1590	0.44	92	0.74
	2000	2211	0.49	181	0.68
3	50	1357	0.23	85	0.73
	2000	1242	0.26	159	0.77
	Inf	1944	0.59	242	0.31
4	20	779	0.12	161	0.55
	50	689	0.43	106	0.51
	2000	940	0.54	155	0.58
5	20	798	0.21	117	0.62
	50	1000	0.33	117	0.70
	2000	900	0.51	141	0.51
6	50	1688	0.32	132	0.69
	200	1236	0.46	141	0.66
	2000	1481	0.42	240	0.65
	Inf	1887	0.66	248	0.32

L-type channel currents may be separated by their characteristic unitary conductances, or where $I_{Ca\text{-}L}$ has been blocked or completely run down.

In several noncardiac cell types a low-threshold Ca^{2+} current has been studied in detail (e.g., Bossu and Feltz, 1986; Carbone and Lux, 1987*a* and *b*; see also Hagiwara et al., 1988, for studies in sino-atrial node cells). These low-threshold Ca^{2+} currents are transient and have voltage-dependence and pharmacological characteristics resembling $I_{Ca\text{-}T}$, suggesting that they may be the same channel type. While it is tempting to identify the cardiac T-type Ca^{2+} channel with similar channels in other cell types, this will require more detailed physical and biochemical comparisons. It seems clear, however, that these channels share numerous similarities.

Kinetic characteristics of $I_{Ca\text{-}T}$

These studies indicate that $I_{Ca\text{-}T}$ has a complex kinetic behavior. The experimental observations of importance are: (*a*) $I_{Ca\text{-}T}$ appears to inactivate completely at all voltages tested. The current decay may be fitted by a single exponential, except just above threshold voltage. It decays faster at more depolarized potentials and the decay is not altered by Ca^{2+}. (*b*) The time course of onset of steady-state inactivation required more than one exponential. A fast phase of inactivation was prominent at voltages where activation of $I_{Ca\text{-}T}$ was prominent, and inactivation tended to follow the time course of $I_{Ca\text{-}T}$ decay. A slow phase of inactivation was seen at all voltages, and was prominent at near-threshold voltages. (*c*) In the subthreshold voltage range, there was a suggestion of a lag in the onset of inactivation. (*d*) Recovery from inactivation showed a fast component and a slow component, and it could be fitted by two exponential functions. The fast recovery component was prominent after a brief inactivating step, and the slow recovery component grew in relative size as the inactivation step was prolonged. Both recovery components were faster at more hyperpolarized voltages, and there was no dependence on Ca^{2+}. (*e*) Onset of recovery showed a lag that was prominent after long inactivating steps.

Inactivation

The $I_{Ca\text{-}T}$ decay was found to be well fitted by a single exponential (see also Hagiwara et al., 1988). Similar findings have been reported by Bossu and Feltz (1986) and by Carbone and Lux (1987*a*) for the low-threshold Ca^{2+} current in rat sensory neurons. These investigators also showed similar voltage dependence to that seen for the cardiac $I_{Ca\text{-}T}$. Bossu and Feltz (1986) showed two components of onset of inactivation, which varied with membrane potential. The lag in the onset of inactivation seen in our experiments at subthreshold voltages was not reported by these two groups of investigators, but it is consistent with the suggestion of Carbone and Lux (1987*b*) that inactivation is at least partially coupled to activation. $I_{Ca\text{-}L}$ is also described to have a complex onset of inactivation, with one component attributed to voltage and the second to Ca^{2+} interacting with some site near the inner channel mouth (see Eckert and Chad, 1984, for review). In agreement with Carbone and Lux (1987*a*), we found that the two inactivation components of $I_{Ca\text{-}T}$ are not sensitive to Ca^{2+}, because Ba^{2+} currents show identical behavior. It seems clear that, although inactivation of $I_{Ca\text{-}T}$ is complex, it is entirely voltage dependent in these cardiac and nerve cells.

It is likely that $I_{Ca\text{-}T}$ channels can inactivate without opening. We found that slow inactivation occurred in the absence of any discernable activation of current. This suggests that a kinetically slow transition may be made from closed to inactivated state(s). When steps were made to more depolarized potentials, where current was activated, a rapid phase of inactivation from the open state was seen. It is possible that our experiments showing slow inactivation without activation were misleading. Near threshold voltage, activation of current may have been sufficiently slow so that it could not be resolved by our current-recording system. Near threshold voltage, Carbone and Lux (1987*b*) demonstrated by single channel recording the presence of a large number of null sweeps, and they concluded that the low-threshold Ca^{2+} channels also can inactivate without opening. Comparable single channel studies of cardiac $I_{Ca\text{-}T}$ channels are not yet available.

Recovery from inactivation

Recovery of $I_{Ca\text{-}T}$ from inactivation could be fitted as a biexponential process, and after a brief-duration inactivating step most current recovered rapidly. For 50-ms-long inactivating steps, 60–80% of the current recovered at -80 mV with a time constant of $\sim$100 ms, the remainder recovering with a time constant of 1–2 s. Longer inactivating steps increased the slow component of recovery, concomitant with a reduction in the fast phase, but with little change in the time constants of the two processes. The time course also was slowed by allowing recovery at a more depolarized potential (Fig. 5).

Although $I_{Ca\text{-}T}$ was inactivated at the end of depolarizing steps of 50 ms duration or more, a change in the inactivated state must have occurred during more prolonged depolarized potentials so that recovery progressively slowed from that encountered in the initial state. This behavior resembles that reported for sensory neurons by Bossu and Feltz (1986). Our results, however, do not support their conclusion that the two components of recovery are independent processes and that slow component had characteristics of a Ca^{2+}-mediated process. Bossu and Feltz (1986, see their Fig. 3) were not always able to show that recovery required more than one exponential and they interpreted this as evidence for separable recovery processes. In contrast, regardless of the duration of the initial depolarizing step we used in our cells, both phases of recovery always were present, suggesting that the two recovery processes could not be separated. Dependence of recovery on Ca^{2+} cannot explain the protocol dependence of recovery we found because Ca^{2+} entry during the initial inactivating step should be identical for steps of 50 ms duration or longer, and replacement of Ca^{2+} by Ba^{2+} did not alter recovery. Thus, for cardiac $I_{Ca\text{-}T}$, recovery from inactivation follows complex kinetics behavior that seems to depend on voltage but not Ca^{2+}.

Yatani et al. (1983) described similar biexponential recovery behavior for $I_{Ca\text{-}L}$ in snail neurons, and this behavior was not dependent on Ca^{2+}. Lengthening the duration of the activating pulse increased the contribution of the slow phase of recovery, but the value of the time constants they obtained were unchanged. They found no delay in the onset of recovery which led them to propose a model where two inactivated states existed in a parallel configuration.

Comparison with Na^+ channel kinetics

Many of the kinetic characteristics of $I_{Ca\text{-}T}$ resemble qualitatively those that have been described for the Na^+ channel (French and Horn, 1983; Horn and Vandenberg, 1984; Fozzard et al., 1985). Ebihara et al. (1983; see also Follmer et al., 1987) described recovery of cardiac I_{Na} from inactivation to be a two-component process, dependent on the duration of the inactivating step. Short (<50 ms) inactivating steps were followed by rapid recovery that for I_{Na} could be well described by a single exponential. However, longer inactivating steps were followed by the appearance of a slowly recovering component that became larger with longer inactivating steps. A delay in the onset of recovery of I_{Na} has been described for nerve (Chiu, 1977) and cardiac (Fozzard et al., 1984; Follmer et al., 1987) cells. Similarly, a delay in the onset of inactivation has been reported in I_{Na} of nerve (Bezanilla and Armstrong, 1977; Bean, 1981) and heart (Mitsuiye and Noma, 1987). Although the channel types differ markedly in their quantitative behavior, the qualitative similarity of $I_{Ca\text{-}T}$ and I_{Na} kinetics suggests that it may be possible to describe the T-type Ca^{2+} channel with kinetic models similar to those models used to describe Na^+ channel kinetics.

A kinetic model

Carbone and Lux (1987*b*) have proposed a Markov chain model for the low-threshold Ca^{2+} channel. They found evidence for two open states based on two single channel conductance levels, but the kinetics of these two states appeared to be the same. If the kinetics are the same, then we could not separate two open states in our experiments, and we can assume only one open state for purposes of our kinetic analysis.

Recovery in the Carbone and Lux (1987*b*) model could be a first order process without a lag, because it would be transitions from an inactivated state to closed states. The model proposed by Chiu (1977) to explain complex inactivation of Na^+ channels in myelinated nerve would qualitatively imitate the inactivation and recovery behavior we observe for $I_{Ca\text{-}T}$. This model, shown in Fig. 8 (*left*), introduces multiple inactivated states in series, one accessed by both C and O states (I_1) and an additional state(s) (I_n) accessed only from I_1. Development of inactivation would proceed slowly at subthreshold (i.e., negligible $C \rightarrow O$ transitions) potentials, where $C \rightarrow I$ is slow. More depolarized potentials favor $C \rightarrow O$ and the development of current, and adds inactivation by $O \rightarrow I$. With inactivation, there is a slow development of a steady-state distribution between I_1 and I_n. Recovery after most of the channels have entered the I_n state(s) would occur with a

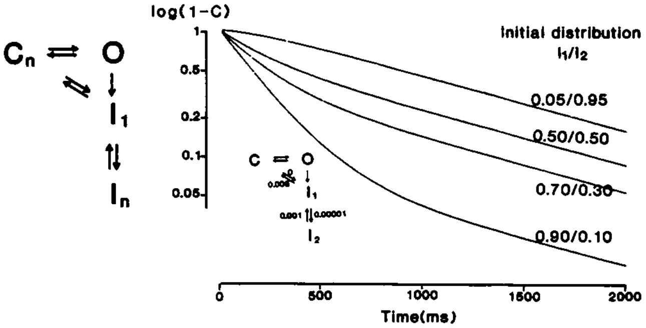

FIGURE 8 Recovery from inactivation: a numerical solution. A general kinetic scheme for the cardiac T-type Ca^{2+} channel is shown to the left (see text for description). The plot shows the time course of recovery from inactivation calculated for different initial distributions of channels between two inactivated states in series (I_1/I_2). The rate constants are shown in the inset. With most channels in I_1 (simulated short-duration inactivating step), recovery was rapid. When channels were primarily in I_2, the state from which they enter and leave slowly (simulated long-duration inactivating step), recovering from inactivation slowed and its onset occurred after a delay. See experimental data in Figs. 5–7.

lag and not as single phase. More than one closed state (C_n) are included to account for the delay in the onset of inactivation.

This model was tested for the kinetic behavior of recovery from inactivation by numerical solutions of the arrival of C as an indicator of recovery, and results are plotted in Fig. 8. Initial conditions were varied to assume four different distributions between two inactivated states (I_1 and I_2) that result from different duration inactivating voltage steps. Longer inactivating steps favor an increase in the fraction of channels in I_2, the inactivated state that channels enter and leave slowly. Inactivated channels were then allowed to recover to C (plotted as log[1 − C]). All channels were assumed to have left C and O, and the transition from C ⟶ I was ignored because this step was shown to be kinetically slow. Rate constants (k_{I1I2}, k_{I2I1}, and k_{I1C}, see inset) were chosen arbitrarily to approximate experimental observations. Recovery was a double exponential process, and an increase in the ratio of channels to favor I_2 resulted in dramatic slowing of the recovery time course and produced in lag in the onset of recovery. This model confirms that a simplified model containing two inactivated states in series reproduces qualitatively the recovery pattern for $I_{Ca\text{-}T}$ (compare model results in Fig. 8 to experimental results in Fig. 7).

In summary, $I_{Ca\text{-}T}$ is relatively large in cardiac Purkinje cells, permitting studies of its kinetic properties. Inactivation and recovery from inactivation of $I_{Ca\text{-}T}$ are complex voltage-dependent processes, similar to the behavior of a low-threshold Ca^{2+} current in sensory neuronal cells. This can be modeled by introduction of two inactivated states in series. The behavior is characterized by rapid recovery of $I_{Ca\text{-}T}$ after brief inactivating depolarizations, and progressively slower recovery with a lag in its onset after long inactivating depolarizations.

Physiological role of cardiac $I_{Ca\text{-}T}$

The physiological role of $I_{Ca\text{-}T}$ in heart cells remains uncertain. The strongest evidence is that $I_{Ca\text{-}T}$ participates in pacemaking in sino-atrial node and possibly other cells (Hagiwara et al., 1988). It also has been suggested that $I_{Ca\text{-}T}$ may participate in certain types of arrhythmogenic afterdepolarizations (January and Fozzard, 1988) and also in slow conduction in some partially depolarized or ischemic tissues (Carmeliet, 1988).

Because $I_{Ca\text{-}T}$ is large in some types of cardiac cells (see Hirano et al., 1989), it also could contribute in these cells to Ca^{2+} loading and to triggering contraction. Lengthening the duration of a voltage clamp step in cardiac Purkinje fibers speeds the time course of restitution of subsequent contractions (Gibbons and Fozzard, 1975). In contrast, our results show that lengthening the duration of an inactivating step slows recovery of $I_{Ca\text{-}T}$. Findings such as these are not consistent with $I_{Ca\text{-}T}$ being the principal mechanism for regulating cardiac contraction. In the presence of other regulatory mechanisms (i.e., $I_{Ca\text{-}L}$, Na-Ca exchange), however, entry of Ca^{2+} through T-type channels may still modify Ca^{2+} regulation by the sarcoplasmic reticulum and contraction. Additional study of the role of $I_{Ca\text{-}T}$ in these mechanisms is required.

This work was supported by National Heart, Lung, and Blood Institute grants HL 20592 and HL 38927.

Received for publication 28 April 1989 and in final form 21 July 1989.

REFERENCES

Bean, B. P. 1981. Sodium channel activation in the crayfish giant axon. Must channels open before inactivating? *Biophys. J.* 35:595–614.

Bezanilla, F., and C. M. Armstrong. 1977. Inactivation of the sodium channel. I. Sodium current experiments. *J. Gen. Physiol.* 70:549–566.

Bossu, J. L., and A. Feltz. 1986. Inactivation of the low-threshold transient calcium current in rate sensory neurones: evidence for a dual process. *J. Physiol. (Lond.)*. 375:341–357.

Bossu, J. L., A. Feltz, and J. M. Thomann. 1985. Depolarization elicits two distinct calcium currents in vertebrate sensory neurons. *Pfluegers Arch. Eur. J. Physiol.* 403:360–368.

Carbone, E., and H. D. Lux. 1987*a*. Kinetics and selectivity of a low-voltage-activated calcium current in chick and rat sensory neurones. *J. Physiol. (Lond.)*. 386:547–570.

Carbone, E., and H. D. Lux. 1987*b*. Single low-voltage-activated calcium channels in chick and rat sensory neurones. *J. Physiol. (Lond.)*. 386:571–601.

Carmeliet, E. 1988. Role of calcium channels in cardiac arrhythmias. *In The Calcium Channel: Structure, Function and Implications.* M. Morad, W. Nayler, S. Kazda, and M. Schramm, editors. Springer-Verlag, Berlin. 310–316.

Chiu, S. Y. 1977. Inactivation of sodium channels: second order kinetics in myelinated nerve. *J. Physiol. (Lond.).* 273:573–596.

Dupont, J.-L., J.-L. Bussu, and A. Feltz. 1986. Effect of internal neurones. *Pfluegers Arch. Eur. J. Physiol.* 406:433–435.

Ebihara, L., N. Shigeto, M. Lieberman, and E. A. Johnson. 1983. A note on the reactivation of the fast sodium current in spherical clusters of embryonic chick heart cells. *Biophys. J.* 42:191–194.

Eckert, R., and J. E. Chad. 1984. Inactivation of calcium channels. *Prog. Biophys. Mol. Biol.* 44:215–267.

Fedulova, S. A., P. G. Kostyuk, and N. S. Veselovsky. 1985. Two types of calcium channels in the somatic membrane of new-born rat dorsal root ganglion neurones. *J. Physiol. (Lond.).* 359:431–446.

Follmer, C. H., R. E. TenEick, and J. Z. Yeh. 1987. Sodium current kinetics in cat atrial myocytes. *J. Physiol. (Lond.).* 384:169–197.

Fox, A. P., M. C. Nowycky, and R. W. Tsien. 1987*a*. Kinetic and pharmacological properties distinguish three types of calcium currents in chick sensory neurones. *J. Physiol. (Lond.).* 394:149–172.

Fox, A. P., M. C. Nowycky, and R. W. Tsien. 1987*b*. Single channel recordings of three types of calcium channels in chick sensory neurones. *J. Physiol. (Lond.).* 394:173–200.

Fozzard, H. A., I. Friedlander, C. T. January, J. C. Makielski, and M. F. Sheets. 1984. Second-order kinetics of Na^+ channel inactivation in internally dialysed canine cardiac Purkinje cells. *J. Physiol. (Lond.).* 353:72P. (Abstr.)

Fozzard, H. A., C. T. January, and J. C. Makielski. 1985. New studies of excitatory sodium currents in heart muscle. *Circ. Res.* 56:475–485.

French, R. J., and R. Horn. 1983. Sodium channel gating: models, mimics, and modifiers. *Annu. Rev. Biophys. Bioeng.* 12:319–356.

Gibbons, W. R., and H. A. Fozzard. 1975. Relationships between voltage and tension in sheep cardiac Purkinje fibers. *J. Gen. Physiol.* 65:345–365.

Gillespie, J. I., and H. Meves. 1980. The time course of sodium inactivation in squid giant axons. *J. Physiol. (Lond.).* 299:289–307.

Hagiwara, N., H. Irisawa, and M. Kameyama. 1988. Contribution of two types of calcium currents to the pace-maker potentials of rabbit sino-atrial node cells. *J. Physiol. (Lond.).* 395:233–253.

Hamill, O. P., A. Marty, E. Neher, B. Sakmann, and F. J. Sigworth. 1981. Improved patch-clamp techniques for high-resolution current recording from cells and cell-free membrane patches. *Pfluegers Arch. Eur. J. Physiol.* 391:85–100.

Hirano, Y., C. T. January, and H. A. Fozzard. 1988. Inactivation of T-type calcium current in cardiac Purkinje cells. *Biophys. J.* 53:554a. (Abstr.)

Hirano, Y., H. A. Fozzard, and C. T. January. 1989. Characteristics of L- and T-type Ca^{2+} currents in canine cardiac Purkinje cells. *Am. J. Physiol.* 256 (*Heart Circ.* 25):H1478–H1492.

Horn, R., and C. A. Vandenberg. 1984. Statistical properties of single sodium channels. *J. Gen. Physiol.* 84:505–534.

January, C. T., and H. A. Fozzard. 1988. Delayed afterdepolarizations in heart muscle: mechanisms and relevance. *Pharmacol. Rev.* 40:219–227.

Kass, R. S., and M. C. Sanguinetti. 1984. Inactivation of calcium channel current in the calf cardiac Purkinje fiber: evidence for voltage- and calcium-mediated mechanisms. *J. Gen. Physiol.* 84:705–726.

Lee, K. S., E. Marban, and R. W. Tsien. 1985. Inactivation of calcium channels in mammalian heart cells: joint dependence on membrane potential and intracellular calcium. *J. Physiol. (Lond.).* 364:395–411.

Mitsuiye, T., and A. Noma. 1987. Inactivation of the guinea-pig cardiac Na channel as examined by the new oil-gap method. *J. Physiol. (Lond.).* 394:42P. (Abstr.)

Nowycky, M. C., A. P. Fox, and R. W. Tsien. 1985. Three types of neuronal calcium channel with different calcium agonist sensitivity. *Nature (Lond.).* 316:440–442.

Provencher, S. W. 1976. A Fourier method for the analysis of exponential decay curves. *Biophys. J.* 16:27–41.

Sheets, M. F., C. T. January, and H. A. Fozzard. 1983. Isolation and characterization of single canine Purkinje cells. *Circ. Res.* 53:544–548.

Tseng, G.-N. 1988. Ca current reactivation in mammalian ventricular myocytes is modulated by intracellular Ca. *Circ. Res.* 63:468–482.

Yatani, A., D. L. Wilson, and A. M. Brown. 1983. Recovery of Ca currents from inactivation: the roles of Ca influx, membrane potential and cellular metabolism. *Cell. Mol. Neurobiol.* 3:381–395.